International Journal of Research in Engineering and Science (IJRES)
ISSN (Online): 2320-9364, ISSN (Print): 2320-9356
www.ijres.org Volume 10 Issue 10 ǁ October 2022 ǁ PP. 593-601

Over-Current Relay Tripping Coordination in A Power System With High Level Of Distributed Generation (Dg) Considering Islanding Mode

Mgbeike V. O[1], Ezechukwu O. A[2], Ezendiokwelu C. E[3] and Anionovo E. U[4]
[*1]*Department of Electrical Engineering, Nnamdi Azikiwe University, Awka, Nigeria*
[2]*Department of Electrical Engineering, Nnamdi Azikiwe University, Awka, Nigeria*
[3]*Department of Electrical Engineering, Nnamdi Azikiwe University, Awka, Nigeria*
[3]*Department of Electrical Engineering, Nnamdi Azikiwe University, Awka, Nigeria*
*Corresponding Author:*Mgbeike V. O

Abstract
During dynamic conditions when the utility no longer operate in parallel with the distributed generators (DG), the power system operates in islanded mode which has an impact on the safety of both the utility and the connected loads. This leads to all customer loads connected to the power island to face fluctuations in both voltage and frequency. In this paper, the Umuahia distribution network in the Nigeria power system was modelled and simulated using the ETAP Software and photovoltaic energy as the DG for this work. The short circuit analysis was performed using symmetrical components while the power flow analysis of the network was done by Newton-Raphson method.

Keywords: *Islanding, Tripping, Fluctuations, Relays, Utility, Photovoltaic, Coordination*

Date of Submission: 13-10-2022 Date of acceptance: 28-10-2022

I. INTRODUCTION

Islanding can be of two forms, either intentional islanding that is performed on purpose by the utility to increase the reliability of the network; the other form of islanding is unintentional islanding, it can be expressed in other words as "the loss of mains" and this occurs when the distributed generator is no more operating in parallel with the utility. Thus, it is not connected to the utility due to a protective disconnection operation taking place by one of the protection devices in the network which could be breaker, fuse or automatic recloser. The DG now is left to energise a certain part of the network that is separated from the utility network forming an isolated power island with the DG as the only power source. The difficulties in islanding cases are due to the ability of the DG to generate power while disconnected from the utility, thus the DG is no more controlled by the utility protection devices and continues feeding its own power island. Islanding can occur only if a generator or a group of generators located in the isolated part are capable of sustaining all the loads in that portion of the network. Forming an isolated power island imposes a difficulty in the reconnection of the isolated power island back to the utility network.

Islanding has an impact on the safety of both the utility and the connected loads, all customer loads connected to this power island will face fluctuations in both voltage and frequency, and those fluctuations might cause severe damages as the voltage and frequency at their terminals are deviated than the standard required levels [1]. It is not desirable for a DG to island with any part of the utility system because if a feeder faces an island reclosing operations, the islanded DG will rapidly drift out of phase with the utility system [2]. After another reclose, the utility will be connected out of phase with the isolated power island, in the case of the absence of blocking the reclose or connection to an energised circuit in the control of the breaker control. Allowing the connection might cause a severe damage to the utility equipment.

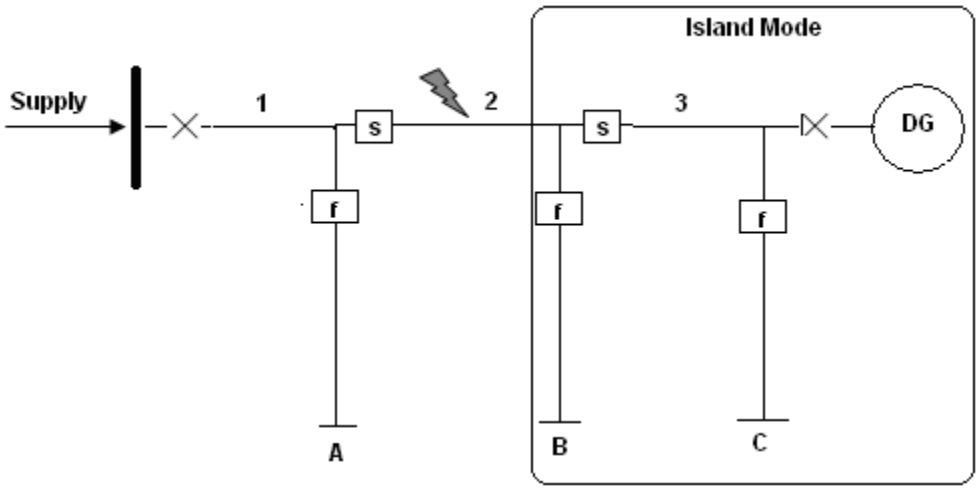

Fig 1: Islanding mode for increasing reliability of DG resource by strategic placement [3].

II. LITERATURE REVIEW

Nowadays the techniques used in detecting islanding situations is by measuring the output parameters of the DG and a decision is taken to decide whether these parameters express an islanding situation or not. Islanding detections methods could be classified in two main groups which are basically active methods and passive methods. The major difference between active and passive methods is that active methods is directly interacting with the power system operation while passive methods are based on identifying the problem based on measured system parameters. Active detection methods realise the islanding situation by measuring the changes in the output power and the system frequency through a designed control circuit providing the necessary variations. During the connection of the DG to the utility, there will be a negligible change occurring in the frequency or power flow that will not be sufficient for the initiation of the protective relay that is responsible for the DG isolation [4]. On the other hand, if the DG is not connected to the utility network, the changes in the frequency and output power will be sufficient enough to energise the relay resulting in the disconnection of the DG preventing the occurrence of an islanding situation. The previously mentioned method will not be efficient in the case of a balance between the loads connected and generation in an islanded part of the network as there will be a non detective zone (NDZ), which is defined as "the island load values for which the detection method fails to detect islanding" [5],[6].

Passive detection methods monitor the variations occurring in the power system parameters such as the short circuit levels, phase displacement and the rate of output power as in most cases of utility disconnection the nominal network voltage, current and frequency are affected. A passive method utilises these changes to decide and react to an islanding situation. Passive methods have the same weakness as the active methods against the insignificant mismatch between the generation and load in islanded part but on the other hand passive methods are less expensive than active methods [7]. During the past few decades, several islanding detection methods were introduced to protect the distribution systems with DG from the case of unintentional islanding. One of the direct and efficient methods is by monitoring the trip status of the main utility circuit breaker and as soon as the main circuit breaker trips, an immediate signal is sent to the circuit breaker at the interconnection between the DG and the utility system to trip the interconnection circuit breaker preventing the occurrence of islanding. Although this method seems to be easy and straight forward, its implementation is so difficult due the distribution of DGs in a large geographic range that will require special comprehensive monitoring techniques with dedicated systems.

The overcurrent (OC) protection strategy requires firstly accurate measurement of fault current magnitude, and then performs comparison with a predefined OC threshold to determine if a fault has occurred. If a fault occurred, then the protection devices must respond in a coordinated manner for fast and selective isolation of the fault anywhere along the feeder and laterals [8], [9]. In [10] the changes in fault currents passing through protection devices when DGs are connected to the system was demonstrated and suggested that protection coordination must be checked after connecting each DG to distribution network. However, this approach is applicable only in the presence of low penetration of DGs into the system. In [11] a conventional OC protection system was assumed to have unidirectional current flow as well as having a fixed pickup setting determined through load flow study. The feeder OC protection system based on this assumption was designed

such that the coordinated switching strategy will be maintained irrespective of change in network condition such as load changes and network topology reconfiguration.

III. MATERIALS AND METHODS

The Umuahia distribution network in the Nigeria power system was modelled using ETAP Software [12]. The impact evaluation of the distribution network operating in islanded mode with photovoltaic energy as the DG was done in this paper, the short circuit analysis was performed using symmetrical components while the power flow analysis of the network was done by Newton-Raphson method.

3.1 Modelling of Umuahia 132/33kV transmission substation

The two bus system with the receiving end voltage as a reference phasor is given as $V_R = |V_R| < 0°$ and the sending end voltage lead it by an angle δ given as $V_s = |V_s| < \delta°$, where δ is the torque angle. The complex power leaving the receiving end and entering the sending end of the transmission line can be expressed per phase in equation (3.1) and (3.2) respectively.

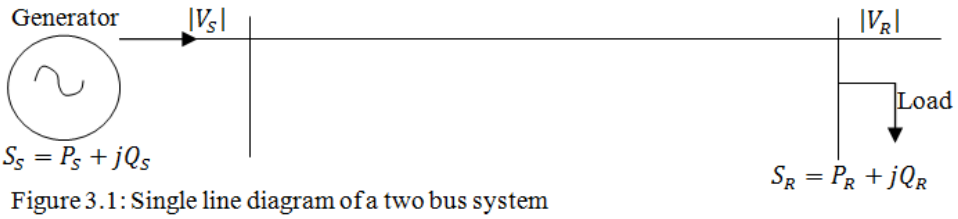

Figure 3.1: Single line diagram of a two bus system

$$S_S = P_S + jQ_S = V_S I_S \quad (3.1)$$

$$S_R = P_R + jQ_R = V_R I_R \quad (3.2)$$

Where I_S, I_R are the sending end and receiving end currents and can be expressed in terms of their sending-end and receiving-end voltages through a transmission line whose equation is given as expressed in eqn (3.3).

$$\begin{bmatrix} V_S \\ I_S \end{bmatrix} = \begin{bmatrix} A & B \\ C & D \end{bmatrix} * \begin{bmatrix} V_R \\ I_R \end{bmatrix} \quad (3.3)$$

And ABCD are the transmission line constraints

S_S = Sending end power — Q_R = Receiving end reactive power
S_R = Receiving end power — V_S = Sending end Voltage
P_S = Sending end real power — V_R = Receiving end Voltage
P_R = Receiving end real power — I_S = Sending end current
Q_S = Sending end reactive power — I_R = Receiving end current

Hence,

$$I_R = \frac{1}{B}V_S - \frac{A}{B}V_R \quad (3.4)$$

$$I_S = \frac{D}{B}V_S - \frac{I}{B}V_R \quad (3.5)$$

Let A, B, D, the transmission line constants, given in equation (3.3) and (3.4) be;

$A = |A| < \alpha, B = |B| < \beta, D = |D| < \alpha \ (since\ A = D)$

Substituting in equation (3.3) and (3.4), we have equations (3.5) and (3.6) as follows:

$$I_R = \left|\frac{1}{B}\right| * |V_S| < (\delta - \beta) - \left|\frac{A}{B}\right| * |V_R| < (\alpha - \beta) \quad (3.5)$$

$$I_S = \left|\frac{D}{B}\right| * |V_S| < (\alpha + \delta - \beta) - \left|\frac{1}{B}\right| * |V_R| < -\beta \quad (3.6)$$

Substituting in equation (3.5) and (3.6), in equations (3.0) and (3.1), we have

$$S_R = |V_S| < 0 \ \left[\left|\frac{1}{B}\right| * |V_S| < (\delta - \beta) - \left|\frac{A}{B}\right| * |V_R| < (\alpha - \beta)\right] \quad (3.7)$$

$$S_{S=} \left|\frac{D}{B}\right| * |V_S|^2 < (\beta - \alpha) - \left|\frac{[V_S]|V_R|}{B}\right| < (\beta + \alpha) \quad (3.8)$$

Then, three phase receiving-end complex power S_R is given by equation (3.9)

$$S_{R(3phase)=} \left|\frac{[V_S]|V_R|}{B}\right| < (\beta - \delta) - \left|\frac{A}{B}\right| * |V_R|^2 < (\beta - \alpha) \quad (3.9)$$

The imaginary parts of equation (3.38) and (3.39) are expressed in equation (3.0) to (3.3)

For receiving end:

$$P_R = \left|\frac{|V_R||V_R|}{B}\right| \cos(\beta - \delta) - \left|\frac{A}{B}\right| * |V_R|^2 \cos(\beta - \alpha) \quad (3.10)$$

$$Q_R = \left|\frac{|V_S||V_R|}{B}\right| \sin(\beta - \delta) - \left|\frac{A}{B}\right| * |V_R|^2 \sin(\beta - \alpha) \quad (3.11)$$

For sending end:

$$P_S = \left|\frac{D}{B}\right| * |V_R|^2 \, cos(\beta - \alpha) \left|\frac{|V_S||V_R|}{B}\right| \cos(\beta + \alpha) \quad (3.12)$$

$$Q_S = \left|\frac{D}{B}\right| * |V_S|^2 \, sin(\beta - \alpha) \left|\frac{|V_S||V_R|}{B}\right| \sin(\beta + \alpha) \quad (3.13)$$

From the above equations P_R will be maximum when $\beta = \delta$

Such that

$$P_{R(max)} = \left|\frac{|V_S||V_R|}{B}\right| - \left|\frac{A}{B}\right| * |V_R|^2 \, cos(\beta - \alpha) \quad (3.14)$$

$$Q_{R(max)} = -\left|\frac{A}{B}\right| * |V_R|^2 \, sin(\beta - \alpha) \quad (3.15)$$

Let A,B,C,D the transmission line constants for a short transmission line given as:

$$\begin{vmatrix} A & B \\ C & D \end{vmatrix} = \begin{vmatrix} 1 & Z \\ 0 & 1 \end{vmatrix} \quad (3.16)$$

Let A,B,C,D the transmission line constants for a medium length line (nominal-π model) given as equation (3.17).

$$\begin{vmatrix} A & B \\ C & D \end{vmatrix} = \begin{bmatrix} (1 + \frac{1}{2}YZ) & Z \\ Y(1 + \frac{1}{4}YZ) & (1 + \frac{1}{2}YZ) \end{bmatrix} \quad (3.17)$$

Where Z= total series impedance and Y =total shunt admittance.

The Umuahia transmission system comprises of several buses which are interconnected by means of power lines. Power is injected into a bus from generator while the loads are tapped from it.

Thus at the i^{th} bus, the net complex power injected into the bus is given by equation (3.18)

$$S_i = P_i + jQ_i = (P_{Gi} - P_{Di}) + j(Q_{Gi} - Q_{Di}) \quad (3.18)$$

While the complex power supplied by the generator is given in equation (3.19)

$$S_{Gi} = P_{Gi} + jQG_i \quad (3.19)$$

And the complex power drawn by the load is given in equation (3.20)

$$S_{Di} = P_{Di} + jQ_{Gi} \quad (3.20)$$

The real and reactive powers injected into the i^{th} bus are given by equation (3.21)

$$P_i = P_{Gi} - P_{Di} \quad i = 1,2,3, \dots \dots, n$$

$$Q_i = Q_{Gi} - Q_{Di} \quad i = 1,2,3, \dots \dots, n \quad (3.21)$$

In a power system each bus is associated with four quantities, real power, reactive power, bus voltage magnitude and its phase angle. In a load flow solution two of the four quantities are specified and the remaining is required to be obtained through the solution of the equations.

IV. RESULTS AND DISCUSSION

Distributed generation units can be operated either grid connected to limit transmission losses and for peak shaving or islanded to avoid total outage when main utility gets interrupted and hence increasing system reliability. For islanded mode, during fault condition the DGs become the only sources of supply without the contribution of the main utility to the loads. A high DG penetration would result in the possibility of operating distribution system in islanded mode which has an issue in conventional over-current protection system and needs a new requirement in protection scheme. The degree of penetration of DG in the system is instrumental to the level of effects it would have to the protection scheme.

4.1 Relay Coordination Analysis for Fault located at Afara 33kV feeder end with 20% DG Penetration considering islanded mode

The results of the relay coordination for 20% distributed generation were done using fault locations at three strategic points on the network for the short circuit fault analysis.

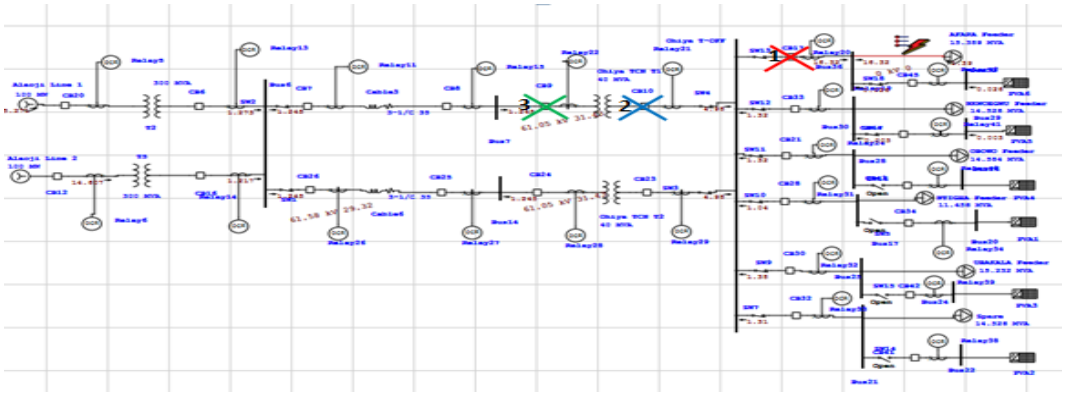

Fig. 4.1: Relay coordination simulation for fault on Afara feeder for 20% DG penetration

Table 4.1: Sequence of operation summary report with Fault at Afara 33kV feeder for 20% DG Penetration

Symmetrical 3-Phase Fault at Afara 33kV feeder for 20% DG Penetration			
Time (ms)	**ID**	**If (kA)**	**Condition**
11.4	R20	2.695	Phase –OC1 – 50
82.8	R21	2.591	Overload Phase – Thermal
87.7	R22	2.475	Phase – OC1 – 50
337	Afara feeder CB		Tripped by R20 Phase – OC1 – 50
345	CB10		Tripped by R21 Overload Phase
389	T1 CB		Tripped by R22 Phase – OC1 – 50

The sequence of operation of relays R20, relay R21and relay R22 for a three-phase symmetrical fault incident on Afara 33kV feeder with 20% DG penetration was shown in Table 4.1. Relay R20 sees a fault of 2.695kA in 0.0114 seconds and then triggers Afara CB to trip on instantaneous overcurrent (OC-50) in 0.337 seconds. At the same instance, relay R21 sees a fault current of 2.591kA in 0.0828seconds and trips CB10 on phase overload in 0.0345seconds while relay R22 sees a fault of 2.475kA in 0.877 seconds and trips T1 secondary CB on instantaneous over current (OC1-50) in 0.389 seconds.

4.2 Case when Fault was located at Afara 33kV feeder end with 50% DG Penetration

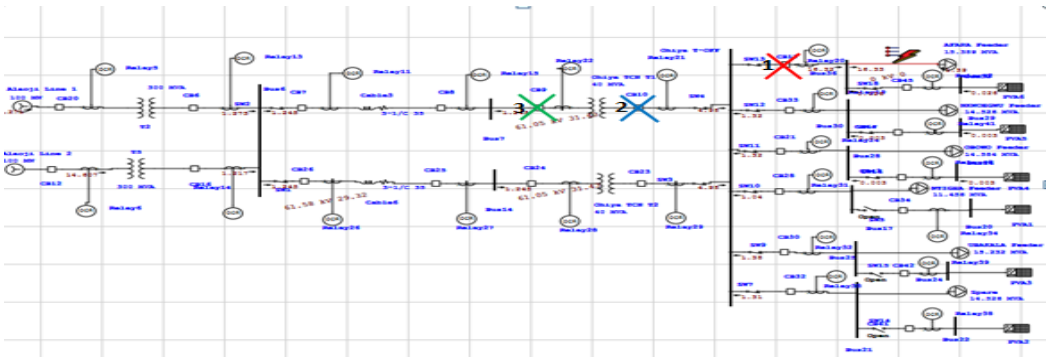

Figure 4.2: Relay coordination simulation for fault on Afara feeder for 50% DG penetration

Table 4.2: Sequence of operation event summary report for 50% DG Penetration

Symmetrical 3-Phase Fault at Afara 33kV feeder for 50% DG Penetration			
Time (ms)	**ID**	**If (kA)**	**Condition**
11.3	R20	2.696	Phase –OC1 – 50
82.7	R21	2.592	Overload Phase – Thermal
87.6	R22	2.476	Phase – OC1 – 50
336	Afara feeder CB		Tripped by R20 Phase – OC1 – 50
344	CB10		Tripped by R21 Overload Phase
388	T1 CB		Tripped by R22 Phase – OC1 – 50

For the three-phase symmetrical fault incident on Afara 33kV feeder with 50% DG penetration, the sequence of operation of relays R20, relay R21and relay R22 was shown in Table 4.2. Relay R20 sees a fault of 2.696kA in 0.0113 seconds and then triggers Afara CB to trip on instantaneous overcurrent (OC-50) in 0.336 seconds. At the same instance, relay R21 sees a fault current of 2.592kA in 0.0827seconds and trips CB10 on phase overload in 0.0344seconds while relay R22 sees a fault of 2.476kA in 0.876 seconds and trips T1 secondary CB on instantaneous over current (OC1-50) in 0.388 seconds.

4.3 Case when Fault was located at Afara 33kV feeder end with 70% DG Penetration

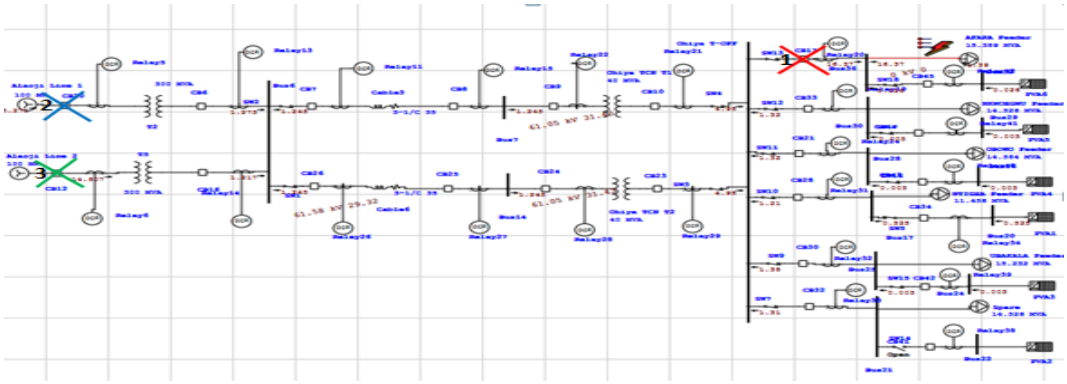

Figure 4.3: Relay coordination simulation for fault on Afara feeder for 70% DG penetration

Table 4.3: Sequence of operation event summary report for 70% DG Penetration

Symmetrical 3-Phase Fault at Afara 33kV feeder for 70% DG Penetration			
Time (ms)	**ID**	**If (kA)**	**Condition**
18.5	R20	1.325	Phase –OC1 – 50
102.3	R5	1.242	Overload Phase – Thermal
107.6	R6	1.135	Phase – OC1 – 50
431	Afara feeder CB		Tripped by R20 Phase – OC1 – 50
429	CB20	1.346	Tripped by R21 Overload Phase
416	CB12	1.349	Tripped by R22 Phase – OC1 – 50

The sequence of operation of relays R20, relay R5 and relay R6 for a three-phase symmetrical fault incident on Afara 33kV feeder with 70% DG penetration was shown in Table 4.3. Relay R20 sees a fault of 1.325kA in 0.0185 seconds and then triggers Afara CB to trip on instantaneous overcurrent (OC-50) in 0.431 seconds. At the same instance, relay R5 sees a fault current of 1.242kA in 0.102 seconds and trips CB20 on phase overload in 0.429 seconds while relay R6 sees a fault of 1.135kA in 0.107 seconds and trips CB10 on instantaneous over current (OC1-50) in 0.416 seconds.

4.4 Case when fault was located at 132kV bus with 20% DG Penetration

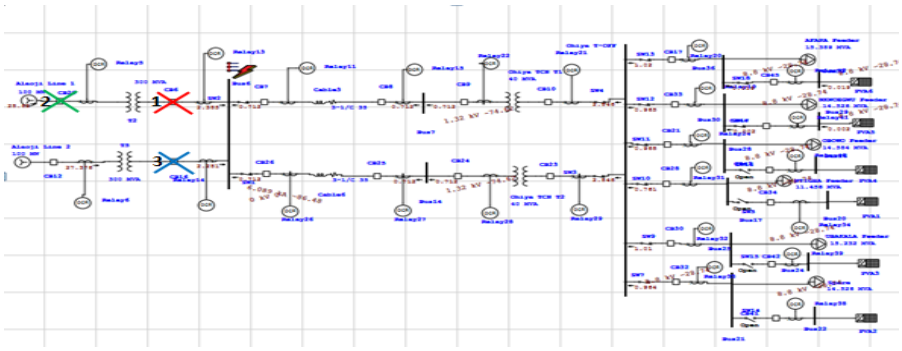

Figure 4.4: Network diagram for fault at 132 kV bus with 20% DG Penetration

Table 4.4: Sequence of operation summary report for fault at 132kV bus with 20% DG Penetration

Symmetrical 3-Phase Fault at 132kV side with 20% DG Penetration			
Time (ms)	**ID**	**If (kA)**	**Condition**
168	R13	2.958	Phase –OC1 – 50
190	R5	2.947	Overload Phase – Thermal
311	R6	2.827	Overload Phase – Thermal
467	CB6		Tripped by R5 Phase – OC1 – 50
590	CB20		Tripped by R6 Overload Phase
634	CB12		Tripped by R13 Overload Phase
1165	R5	2.956	Phase – OC1 – 51
1151	R6	2.958	Phase – OC1 – 51

Table 4.4 shows the sequence of operation of relay R13, R5 and R6 for a three-phase symmetrical fault incident on the 132 kV side with 20% DG penetration. The R13 definite time characteristic (OC1 – 51) time of operation was found to be 0.168 seconds for a fault 2.958 kA which then trips the CB6 in 0.468 seconds. R5 sees a fault of 2.947A at 0.190 seconds which trips the CB20 in 0.590 seconds. Similarly, the R6 definite time relay characteristic (OC – 51) time of operation was found to be 1.311 seconds for a fault of 2.827A which trips the circuit breaker CB12 in 0.634 seconds.

4.5 Case when fault was located at 132kV bus with 50% DG Penetration

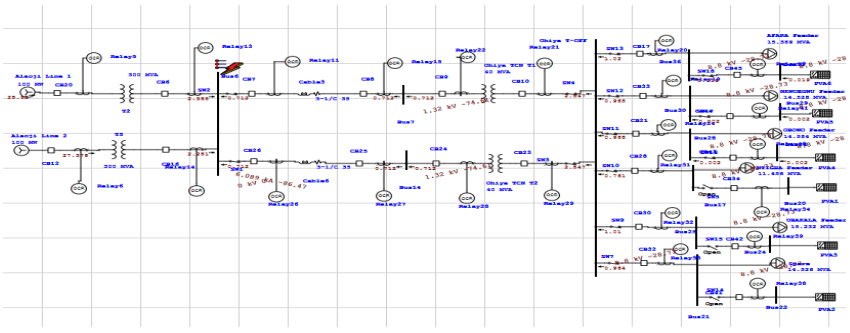

Figure 4.5: Network diagram for fault located at 132 kV bus with 50% DG Penetration

Table 4.5: Sequence of operation summary report for fault at 132kV side with 50% DG Penetration

Symmetrical 3-Phase Fault at 132kV side with 50% DG Penetration			
Time (ms)	**ID**	**If (kA)**	**Condition**
170	R13	2.981	Phase –OC1 – 50
195	R5	2.969	Overload Phase – Thermal
321	R6	2.858	Overload Phase – Thermal
472	CB6		Tripped by R5 Phase – OC1 – 50
598	CB20		Tripped by R6 Overload Phase
647	CB12		Tripped by R13 Overload Phase
1175	R5	2.967	Phase – OC1 – 51
1163	R6	2.978	Phase – OC1 – 51

Table 4.5 shows the sequence of operation of relay R13, R5 and R6 for a three-phase symmetrical fault incident on the 132 kV side with 50% DG penetration. The R13 definite time characteristic (OC1 – 51) time of operation was found to be 0.170 seconds for a fault 2.981 kA which then trips the CB6 in 0.472 seconds. R5 sees a fault of 2.969A at 0.195 seconds which trips the CB20 in 0.598 seconds. Similarly, the R6 definite time relay characteristic (OC – 51) time of operation was found to be 0.321 seconds for a fault of 2.858A which trips the circuit breaker CB12 in 0.647 seconds.

4.6 Case when fault was located at 132kV bus with 70% DG Penetration

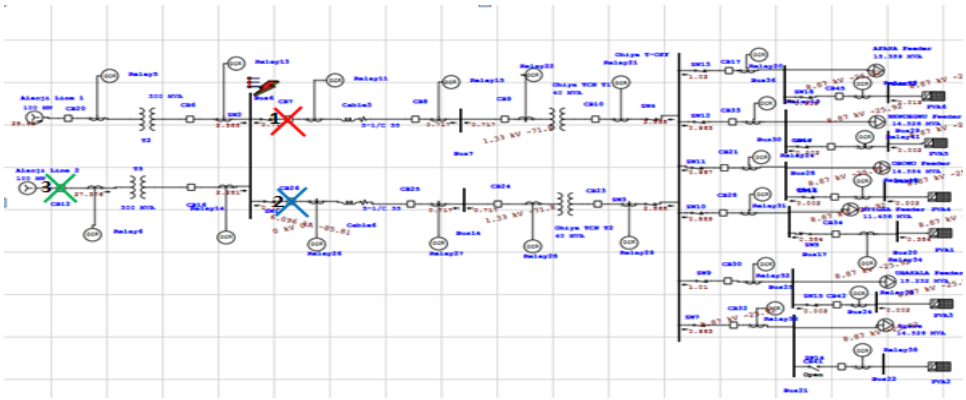

Figure 4.6: Network diagram for fault at 132 kV bus with 70% DG Penetration

Table 4.6: Sequence of operation summary report for fault at 132kV side with 70% DG Penetration

Symmetrical 3-Phase Fault at 132kV side with 70% DG Penetration			
Time (ms)	**ID**	**If (kA)**	**Condition**
210	R11	1.219	Phase –OC1 – 50
243	R26	1.213	Overload Phase – Thermal
415	R6	1.152	Overload Phase – Thermal
482	CB7		Tripped by R5 Phase – OC1 – 50
621	CB26		Tripped by R6 Overload Phase
739	CB12		Tripped by R13 Overload Phase
1218	R26	1.235	Phase – OC1 – 51
1223	R6	1.230	Phase – OC1 – 51

Table 4.6 shows the sequence of operation of relay R11, R26 and R6 for a three-phase symmetrical fault incident on the 132 kV side with 70% DG penetration. The relay R11 definite time characteristic (OC1 – 51) time of operation was found to be 0.210 seconds for a fault 1.219 kA which then trips the CB7 in 0.482 seconds. R26 sees a fault of 1.213A at 0.243 seconds which trips the CB26 in 0.621 seconds. Similarly, the R6 definite time relay characteristic (OC – 51) time of operation was found to be 0.415 seconds for a fault of 1.152A which trips the circuit breaker CB12 in 0.739 seconds.

II. CONCLUSION

When the level of DG penetration was gradually increased from 20% to 70% for faults at Afara 33kV feeder and 132kV side considering Islanded mode, it was observed that for 20% DG penetration the sequence of operation showed correct fault current measurement, accurate tripping time for the relays and correct coordination for the circuit breakers. This accurate tripping and good coordination was also observed for conditions when there was fault at the 132kV side for 20% DG penetration. Also for 50% DG penetration, the tripping time of the relays were delayed and slightly affected due to lower values of fault current seen by the relays but this did not affect the tripping coordination of the circuit breaker. During high penetration of DG, the sequence of operation results for faults at different locations with 70% DG penetration showed that the system operated in islanded mode. It was observed that the fault current was affected due to the high DG insertion in the distribution system. Since the fault current depends on the source MVA short circuit level and during this mode the DGs are the only source of supply, the fault current was seen to be very low that it affected the tripping time and relay coordination for cases of fault in all location.

REFERENCES

[1] Redfern, M. A., & Usta, O. (1995, July). A new microprocessor based islanding protection algorithm for dispersed storage and generation units. IEEE Transaction on Power Delivery, 10(4), 1249-1254.

[2] Urdal, H., Ierna, R., Zhu, J., Ivanov, C., Dahresobh, A., & Rostom, D. (2015) "System strength considerations in a converter dominated power system," IET Renewable Power Generation, 9(1), 10-17.

[3] Ropp, M. E., Begovic, M., Rohatgi, A., Kern, G. A., Bonn, R. H., & Gonzalez, S. (2000, September). Determining the relative effectiveness of islanding detection methods using phase criteria and non detection zones. IEEE Transaction on Energy Conversion, 15(6), 290-296.

[4] Pai, F. S., & Huang, S. J. (2001, December). A detection algorithm for islanding prevention of dispersed consumer owned storage and generating units. IEEE Transaction on Energy Conversion, 16(3) 346-351.

[5] Abyaneh, H. A., Al-Dabbagh, M., Karegar, H. K., Sadeghi, S. H., & Khan, R. A. (2003, April). A new optimal approach for coordination of overcurrent relays in interconnected power systems. IEEE Transaction on Power Delivery, 18(8), 430-435.

[6] Urdaneta, A. J., Perez, L. G., & Restrepo, H. (1997, October). Optimal coordination of directional overcurrent relays considering dynamic changes in the network topology. IEEE Transaction on Power Delivery, 12(5), 1458-1464.

[7] Urdaneta, A. J., Nadira, R., & Perez, L. G. (1998, July). Optimal coordination of directional overcurrent relays in interconnected power systems, IEEE Transaction on Power Delivery, 3(2), 903-911.

[8] Wheeler, K. A., Faried, S. O., & Elsamahy, M. (2016). Assessment of distributed generation influences on fuse-recloser protection systems in radial distribution networks. Transmission and Distribution Conference and Exposition (T&D), 2016 IEEE/PES, 1-5.

[9] Mohammadi P., & Mehraeen, S. (2017). Challenges of PV integration in low-voltage secondary networks. IEEE Transactions on Power Delivery, 32(1) 525-535.

[10] Hadjsaid, N., Canard, J. F., & Dumas, F. (1999). Dispersed generation impact on distribution networks. Computer Applications in Power, IEEE, 12(7), 22-28.

[11] Madani, S. M. (1999). Analysis and design of power system protections using graph theory. Technische Universiteit Eindhoven. https://doi.org/10.6100/IR523152

[12] Mgbeike V. O, Ezechukwu O. A, Ezendiokwelu C. E, & Nwoye A. N.(2022, October). Analysis of the Effects of Renewable Energy-Distributed Generation in a Distribution Network. International Journal of Innovative Research in Engineering & management, 9(5), 1-10. https://doi.org/10.55524/ijirem.2022.9.5.1